

RESEARCH ARTICLE

Polymers for Traveling Wave Ion Mobility Spectrometry Calibration

Quentin Duez,^{1,2} Fabien Chiro, ³ Romain Liénard,^{1,4} Thomas Josse,^{1,4} ChangMin Choi,⁵ Olivier Coulembier,⁴ Philippe Dugourd,⁵ Jérôme Cornil,² Pascal Gerbaux,¹ Julien De Winter¹

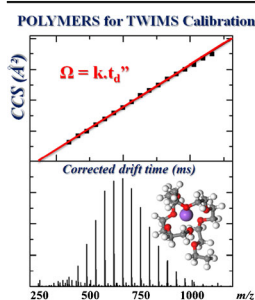
¹Organic Synthesis and Mass Spectrometry Laboratory, Interdisciplinary Center for Mass Spectrometry (CISMa), University of Mons (UMons), Place du Parc, 23, Mons, 7000, Belgium

²Laboratory for Chemistry of Novel Materials, Center of Innovation and Research in Materials and Polymers (CIRMAP), University of Mons (UMons), Place du Parc, 23, Mons, 7000, Belgium

³Université Lyon, Université Claude Bernard Lyon 1, ENS de Lyon, CNRS, Institut des Sciences Analytiques, UMR 5280, 5 rue de la Doua, F-69100, Villeurbanne, France

⁴Laboratory of Polymeric and Composite Materials, Center of Innovation and Research in Materials and Polymers (CIRMAP), University of Mons, UMons, 23 Place du Parc, 7000, Mons, Belgium

⁵Université Lyon, Université Claude Bernard Lyon 1, CNRS, Institut Lumière Matière, F-69622, Lyon, France



Abstract. One of the main issues when using traveling wave ion mobility spectrometry (TWIMS) for the determination of collisional cross-section (CCS) concerns the need for a robust calibration procedure built from referent ions of known CCS. Here, we implement synthetic polymer ions as CCS calibrants in positive ion mode. Based on their intrinsic polydispersities, polymers offer in a single sample the opportunity to generate, upon electrospray ionization, numerous ions covering a broad mass range and a large CCS window for different charge states at a time. In addition, the key advantage of polymer ions as CCS calibrants lies in the robustness of their gas-phase structure with respect to the instrumental conditions, making them less prone to collisional-induced unfolding (CIU) than protein ions. In this paper, we present a

CCS calibration procedure using sodium cationized polylactide and polyethylene glycol, PLA and PEG, as calibrants with reference CCS determined on a home-made drift tube. Our calibration procedure is further validated by testing the polymer calibration to determine CCS of numerous different ions for which CCS are reported in the literature.

Keywords: Polymers, Ion mobility, Traveling wave ion mobility, TWIMS, Calibration

Received: 2 May 2017/Revised: 30 June 2017/Accepted: 9 July 2017/Published Online: 31 July 2017

Introduction

Ion mobility spectrometry (IMS) is increasingly used in the mass spectrometry community for probing the 3D structures of gaseous ions [1]. This methodology allows for the temporal separation of ions based on their mobility in a cell filled with a buffer gas under the influence of an electric field. The drift time

(t_D) of the ions is proportional to their rotationally averaged collision cross-section (CCS) which roughly reflects their three-dimensional shape in the gas phase [1, 2]. Although the concept of ion mobility instrumentation and its coupling with mass spectrometry (IMMS) date from the 60s, recent commercialization of IMMS instruments results in a rapid increase of peer-reviewed publications exploiting the versatility of this technique to study a wide range of compounds such as proteins, synthetic macromolecules, natural products, or host–guest systems [3–7].

Drift tube (DTIMS) and traveling wave (TWIMS) ion mobility spectrometry are the most commonly encountered IMMS systems since they are both commercially available, often

Electronic supplementary material The online version of this article (doi:10.1007/s13361-017-1762-4) contains supplementary material, which is available to authorized users.

Correspondence to: Julien De Winter; e-mail: Julien.dewinter@umons.ac.be

coupled with ToF mass analyzers. Commercial instruments are usually used with N₂ in the mobility cell, although CCS obtained in He are preferable for correlation with theoretical calculations [8]. In the case of a homogenous electric field-based setup in DTIMS, the CCS can be directly determined from the drift time measurements using Equation 1 adapted from the Mason-Schamp relation [8]. In this equation, Ω is the CCS for ions of mass-to-charge ratio m/z . t_D denotes the drift time of those ions through a mobility cell of length L filled by a gas of molecular mass m_N at a pressure P and a temperature T , N being the gas density number at standard temperature and pressure, k_B the Boltzmann constant, and e the elementary charge [1, 9, 10].

$$\Omega = \frac{\sqrt{18\pi}}{16} \frac{ze}{\sqrt{k_B T}} \sqrt{\frac{1}{m_I} + \frac{1}{m_N}} \frac{760}{P} \frac{T}{273.2} \frac{1}{N} \frac{t_D E}{L} \quad (1)$$

In principle, the linear relationship between the Ω and t_D in Equation 1 allows determining the so-called absolute CCS from drift time measurements. Practically speaking, the time directly measurable in an IMS measurement is the arrival time t_A , which differs from t_D since it also accounts for the transfer time t_0 from the end of the drift cell to the detector (usually through ion optics and the mass analyzer). This dead time t_0 a priori depends on the instrument geometry and settings, as well as on the mass-to-charge ratio of the ions (Equation 2) and can be experimentally determined (see Experimental Part) [8].

$$t_A = t_D + t_0 \quad (2)$$

In the case of IMMS instruments using a dynamic electric field, such as in TWIMS, the linear relationship between Ω and t_D is no longer applicable. Current mathematical models describe the relation between the ions drift time in a TWIMS and their CCS by a non-linear equation (Equation 3) for which A and B depend on instrumental parameters [1, 3].

$$\Omega = \frac{\sqrt{18\pi}}{16} \frac{ze}{\sqrt{k_B T}} \sqrt{\frac{1}{m_I} + \frac{1}{m_N}} \frac{760}{P} \frac{T}{273.2} \frac{1}{N} A t_D^B \quad (3)$$

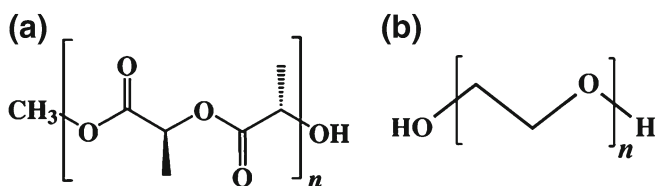
Equation 3 is often rewritten to incorporate all experimental parameters in a new A' factor (Equation 4) where μ stands for the reduced mass for the ion/buffer gas system [1]:

$$\Omega = \frac{z}{\sqrt{\mu}} A' t_D^B \quad (4)$$

From Equations 3 and 4, it immediately appears that the CCS calculation becomes possible from the drift times if the A (or A') and B values are previously determined. This is realized upon establishment of a calibration curve associating CCS to t_D . Such a calibration procedure is built on the measurement of t_D for gaseous calibrant ions of known CCS covering the same charge states and CCS ranges as the analytes. Indeed, the extrapolation

of an unknown nonlinear function is hazardous [11]. Several calibration procedures have already been described in the literature for the CCS determination from t_D measurements on TWIMS. These calibration procedures rely on the use of proteins [1, 12] and peptide mixtures [13–15]. Polyalanine (PolyALA) represents one of the most popular calibrants because of the dispersity of this polymer-like mixture (broad mass and CCS ranges) and its ability to produce ions with different charge states in both positive and negative ion modes [16–18]. PolyALA is also often implemented in commercial software as the default CCS calibration procedure. However, some groups already emphasized that the limited CCS range covered by PolyALA and peptide mixtures represents a drawback of this calibrant [6, 19]. Above all, protein/peptide ions may undergo collision-induced unfolding (CIU), depending on the experimental conditions [21]. The CIU phenomenon that alters the 3D structures of the gaseous calibrant ions renders the calibration procedure highly sensitive to the settings of the instrument, especially using instruments such as a Synapt for which some settings have been reported as highly energetic [20–23]. Sun et al. pointed out that “perfect” CCS calibrant ions are required to exhibit collision-independent properties, in other words they need to be robust (not dependent) to hard instrumental conditions [24]. Nowadays, it becomes of prime importance to identify a standard calibrant solution that will be at the origin of numerous robust CCS calibrant ions with different charge states covering a large range of CCS values.

Based on their intrinsic polydispersities, polymers offer in a single sample the opportunity to generate, upon electrospray ionization, numerous ions covering a broad mass range and a large CCS window for different charge states at a time. Furthermore, we recently demonstrated the robustness of polylactide ions facing a large range of instrumental conditions [25]. In the context of the present work, we will then use complementary synthetic polymers such as α -methyl, ω -hydroxy poly(lactide) (PLA), and poly(ethylene glycol) (PEG) (Scheme 1) to create a large distribution of CCS calibrant ions that will certainly fulfill the aforementioned criteria of “perfect calibrants.” To create the broadest CCS range for different charge states, different polymer samples will be required. We selected PEG samples with average molecular weights (M_n) of 600, 1000, 2000, and 3350 g.mol⁻¹ and PLA samples characterized by average molecular weights of 4000, 5500, and 10,000 g.mol⁻¹. It is important to mention here that all the polymer samples are always analyzed separately and that we never mixed the polymers to end up with a single calibration solution.



Scheme 1. Structures of α -methyl, ω -hydroxy polylactide (a) or poly(ethylene glycol) (b)

The calibration procedure will start by measuring the CCS values of all the polymer ions on a DTIMS experimental setup. This step will be performed using He as the buffer gas since one of the main objectives of the CCS determination is the correlation between experimental and theoretical data. Afterwards, TWIMS measurements will be performed using N₂ as the buffer gas since most of the TWIMS-based setups are run with N₂ instead of He. However, it is worth stressing that our calibration procedure can of course be applied for TWIMS experiments with He. We will demonstrate here that our procedure covers a CCS calibration range larger than the popular PolyALA calibration for five charge states between +1 and +5. The reliability of our calibration procedure will be demonstrated by testing the polymer calibration to determine the CCS of a large panel of ions for which CCS are reported in the literature.

Results and Discussion

Determination of Reference Ω_{Ref} on DTIMS

PLA and PEG samples are envisaged in the present report as potential sources of CCS calibrant ions. It is then first required to accurately determine the CCS of the electrospray-generated ions, named hereafter Ω_{Ref} . Solutions of the synthetic polymer samples are then analyzed on a DTIMS instrument that has been described in detail elsewhere [26, 27]. Figure 1 features the mass spectrum acquired using electrospray ionization in the positive ion mode for a representative PLA sample ($M_n = 4000 \text{ g}\cdot\text{mol}^{-1}$). Here, a discrete distribution of signals is observed for two charge states, namely +3 and +2. One of the main features of the use of polymers as the source of reference ions immediately appears, since all the ions in the mass spectrum can be used as calibrant ions. Consequently, due to their dispersity, only a few polymer samples are required to create a

CCS calibration procedure covering a wide range of CCS for several charge states.

The arrival times for all ions observed in Figure 1 are recorded and corrected by subtracting the dead time (see Experimental Part). The same analysis is also performed for the other PEG and PLA samples and all the Ω_{Ref} are determined and gathered in Supplementary Tables SI 1 to SI 5 for each charge state and degree of polymerization (DP). However, as explained in the following section, some CCS values must be discarded due to the polymer folding phenomena and are therefore not reported in the Supplementary Tables SI 1–5.

Polymer Folding and CCS Values to be Discarded

Several research groups investigated the folding behaviors of multiply cationized polymer ions in the gas phase, with a special emphasis on the evolution of the CCS with the DP [5, 25, 28, 29]. Briefly, it is now well understood that the shortest chains are subjected to the electrostatic repulsion exerted by the presence of numerous cations and appear highly stretched in the gas phase. In the case of longer chains (higher DP), the screening of the Coulombic repulsion by the monomer residues tends to stabilize the cationizing particles. It was also observed that consecutive folding steps are involved on the way to an ultimately globular structure. Each folding step is characterized by the presence of a ‘plateau’ in the evolution of the CCS as a function of the DP (cf. Supplementary Figure SII). Thus, ions with different m/z ratios appear at the same arrival time, making those specific ions no longer compatible with the definition of CCS calibrant ions [5, 25, 28, 29]. Indeed, when used in the calibration procedure presented here below, these ions create inconsistencies in the calibration curve, evidenced by a loop in the curve and a linear regression with a coefficient of determination well below the recommended value of $R^2 = 0.98$

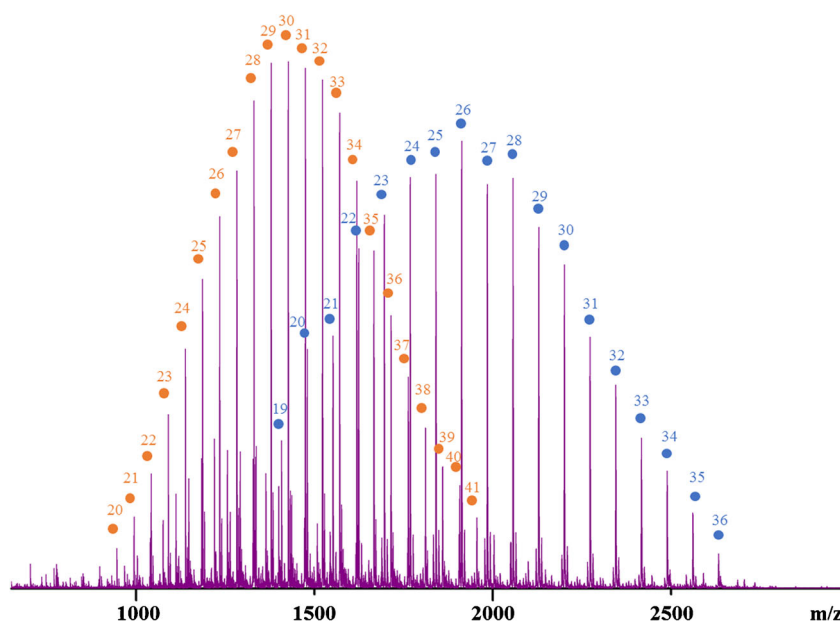


Figure 1. PLA ($M_n \approx 4000 \text{ g}\cdot\text{mol}^{-1}$) mass spectrum recorded with a home-made DTIMS instrument. The orange distribution corresponds to triply charged PLA ions whereas the blue distribution corresponds to doubly charged PLA ions

(Supplementary Figure SI2) [30]. Moreover, our group has recently reported that coexisting folded and unfolded conformers are observed for DP in the plateau region, with the proportion of coexisting conformers being source-dependent [25]. In order to avoid any mistake in the calibration process that may appear by using reported CCS for a given conformer while producing another one using an ionization source with a different geometry, we suggest discarding DPs involved in the folding steps. The discarding of some DPs could a priori shorten the CCS range covered by the calibration but, as shown in the next sections, the combined use of PEG and PLA on the same calibration curve allows interpolating the missing data points.

Description of the Calibration Procedure for the CCS Determination on TWIMS

The proposed calibration procedure is inspired by the methods reported by Forsythe et al. [18] and Robinson et al. [30], and intends to establish a linear relationship between the corrected drift times (t_D'') measured in the TWIMS (N_2) experiments and the CCS_{He} (Ω_{Ref}) for the calibrant ions for a given charge state.

The procedure starts with the determination of the arrival time (t_A) of each calibrant ion on the TWIMS set-up. Arrival times are directly read from the m/z extracted mobilograms at the maximum of the arrival time distribution (ATD). The t_A are then corrected to extract the dead time (t_0) of the Synapt instrument. As described by Forsythe et al. [18] and Robinson et al. [30], the dead time possesses two significant contributions that are (1) the m/z -dependent flight time from the transfer T-wave guide to the pusher, and (2) the time required for ions to fly through the transfer region, time that is considered as m/z -independent. The m/z -dependent contribution is calculated using the 'EDC delay coefficient' (c value) that is instrument-specific and can be found within the control software of the Synapt instrument. This value amounts to 1.51 on the mass spectrometer used in the present study [30]. The time required for ions to transit the transfer region is calculated by taking the length of the transfer T-wave (10 cm) divided by the wave velocity (here 380 $m \cdot s^{-1}$), say 263 μs in the present experimental conditions.

The dead time correction is then described by Equation 5 where t_D' is the corrected drift time, m/z , the ion mass-to-charge ratio, and c , the 'EDC delay coefficient' [30].

$$t_D' = t_A - \left[\frac{c \sqrt{\frac{m}{z}}}{1000} \right] - \frac{\text{Transfer cell length}}{\text{Transfer wave velocity}} \quad (5)$$

As described in [30], the reference Ω_{Ref} must also be corrected to afford a charge- and mass- independent quantity, Ω'_{Ref} [1, 30]. This is achieved by injecting in Equation 6 the

reduced mass of the ion/gas system (μ) and the charge state of the calibrant ion (z).

$$\Omega'_{Ref} = \left[\frac{\Omega_{Ref}}{z} \sqrt{\mu} \right] \quad (6)$$

When associating Equations 5 and 6, we obtain the relationship between Ω'_{Ref} and t_D' presented in Equation 7.

$$\Omega'_{Ref} = A' t_D'^B \quad (7)$$

Equation 7 is best represented using natural logarithm in Equation 8 that expresses a linear relationship, useful to determine the A' and B parameters.

$$\ln \Omega'_{Ref} = B \ln t_D' + \ln A' \quad (8)$$

In particular, the B parameter can be introduced in Equation 9 that allows calculating a new value, t_D'' , which can be directly injected in Equation 4, to afford a linear relationship between the Ω_{Ref} and these newly calculated t_D'' values (Equation 10). Equation 10 represents, for a given charge state, the calibration expression used throughout the manuscript.

$$t_D'' = t_D' \frac{z}{\sqrt{\mu}} \quad (9)$$

$$\Omega_{Ref} = A' t_D'' \quad (10)$$

The proportionality factor A' is obtained from Equation 8. It should be noted that in contrast to Robinson et al. [30] and, considering the shape of Equation 10, the linear fitting goes through the origin $-(0,0)$.

All the polymer samples are then analyzed on the Waters Synapt G2-Si with N_2 as the buffer gas. The t_A of all ions are corrected according to the protocol described here above in order to obtain the t_D'' values (Equations 5–9) [30]. The corrected drift times t_D'' are next plotted as a function of Ω_{Ref} in order to draw the calibration curve for each charge state. As stated above, some DPs have been discarded due to polymer folding issues. Nevertheless, when plotting data obtained from both PEG and PLA samples, a nice linearity is observed and confirmed by the R^2 values for both the charge states +2 and +5 presented in Figure 2. The gap observed in the PEG region for the +2 ions is attributable to the removal of ions of DPs associated with the folding regions.

This linearity allows interpolating a calibration curve such as the one obtained for the +5 polymer ions without any significant error (see CCS determination for ubiquitin and cytochrome *c* in Table 2 and comments below). Calibration curves for other charge states are presented in Supplementary Figure SI 3 and exhibit remarkable linearity as well. Compared

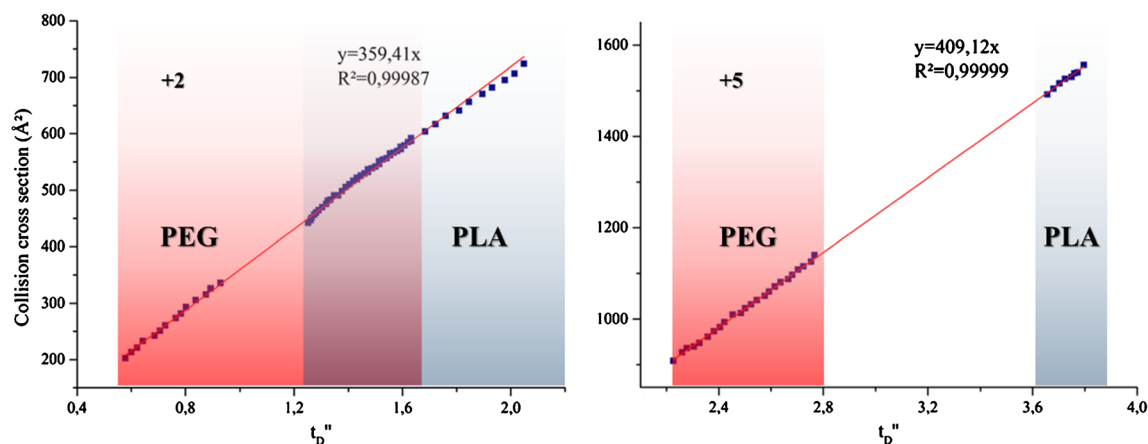


Figure 2. Calibration curves obtained by using polymer calibration for the +2 and +5 charge state ions

with popular calibration procedures such as the standard procedure using PolyALA as calibrant, calibration ranges affordable for each charge state by the polymer calibration are much broader, as schematically presented in Figure 3. However, the PolyALA calibration allows reaching slightly lower CCS values for +1 and +3 ions compared with the present polymer calibration.

Proof of Concept

To validate our calibration procedure, we exposed to TWIMS measurements a large array of analytes, the CCS of which are reported in the literature. The measured t_A are then corrected using Equations 5–9 (cf Part. III) and converted to CCS(He) using the B and A' parameters obtained by the polymer calibration, for each charge state. The so-obtained CCS are then confronted to the literature values to validate the new procedure.

We carefully selected analytes, the CCS of which are in the range covered by the polymer calibration to avoid extrapolation errors. The comparison between CCS determined by our

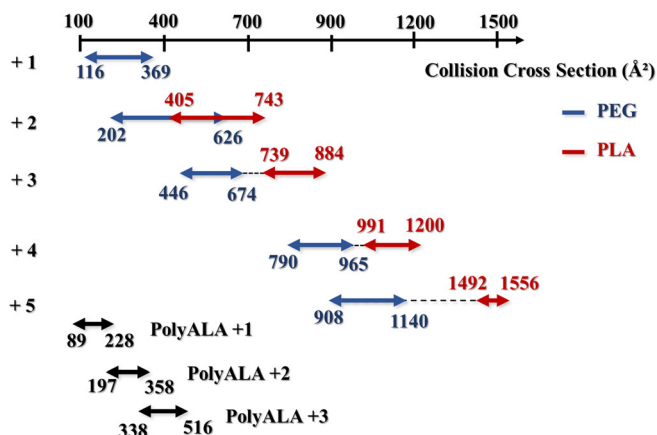


Figure 3. Calibration ranges affordable by the polymer calibration (PEG and PLA ranges are represented separately). As interpolation is acceptable, total calibration ranges for each charge state include the black dashed line. Calibration ranges affordable by the PolyALA calibration are shown for comparison

procedure and reported CCS is presented in Table 1 for +1 and +2 ions and in Table 2 for +3, +4, and +5 ions. Each analysis has been repeated at least four times on different days using diverse IM parameters (Supplementary Table S16 for all the IM sets of parameters) and the presented CCS are mean values, whereas the percentages in brackets are the standard deviation. The differences in percent between the literature CCS and the measured CCS using the polymer calibration are also reported. For CCS that are not reported in the literature (reference *a* in Table 2), the measured CCS using the polymer calibration were compared with the CCS determined on the DTIMS instrument at the University of Lyon in the course of the present study.

From the comparison between reference and measured CCS, we can conclude that our procedure is efficient in reproducing CCS values. Indeed, the average percentage difference between the reference CCS and those determined with the polymer calibration was always lower than 2%, which was a validation criterion used by Bush and al. [16].

Although the polymer calibration has been successfully tested on a large range of collision cross-sections and charge states, we emphasize that this procedure should not be used in extrapolation mode as stated by Shvartsburg et al. [11]. As for a test, we used the +5 melittin ions that have a reference CCS of 613 Å² as reported by Salbo et al. [33]. The +5 polymer calibration range has a lower limit of 908 Å² (Figure 3). If the CCS are tentatively determined on TWIMS using the polymer calibration in extrapolation, a CCS value of 705 Å² is obtained.

Robustness of the Method

To further demonstrate the robustness of polymer ion calibration compared with a protein or peptide ion calibration facing a large range of experimental conditions, PEG and PolyALA ions have been analyzed under two instrumental conditions by modifying the trap bias voltage that is known to energize the ions upon injection from the trap to the ion mobility cells, yielding to either decomposition or isomerization. Two trap bias voltages have been used (i.e., 30 and 110 V). Arrival time

Table 1. Literature CCS Compared with CCS Obtained by the Polymer Calibration for Singly and Doubly Charged Analytes

Charge state	Analyte	Collision cross-section (\AA^2)				
		Polymer calibration CCS	Reference CCS	Reference	Percentage difference (%)	
+1	Reserpin	182 ($\pm 0.7\%$)	179 ($\pm 0.1\%$)	[31]	1.7	
	Bradykinin	245 ($\pm 0.6\%$)	242	[32]	1.2	
	Tetrapentylammonium	134 ($\pm 1.1\%$)	134 ($\pm 0.0\%$)	[31]	0	
	Tetrahexylammonium	153 ($\pm 0.8\%$)	155 ($\pm 0.2\%$)	[31]	1.3	
	Tetraheptylammonium	172 ($\pm 0.9\%$)	175 ($\pm 0.5\%$)	[31]	1.7	
	Tetraoctylammonium	190 ($\pm 1\%$)	194 ($\pm 0.0\%$)	[31]	2.1	
	PolyALA DP8	163 ($\pm 0.9\%$)	157 ($\pm 3\%$)	[16]	3.8	
	PolyALA DP9	176 ($\pm 1.7\%$)	170 ($\pm 3\%$)	[16]	3.5	
	PolyALA DP10	188 ($\pm 1.5\%$)	181 ($\pm 3\%$)	[16]	3.9	
	PolyALA DP11	200 ($\pm 1.6\%$)	194 ($\pm 3\%$)	[16]	3.1	
	PolyALA DP12	212 ($\pm 1.3\%$)	206 ($\pm 3\%$)	[16]	2.9	
	PolyALA DP13	224 ($\pm 1.3\%$)	217 ($\pm 3\%$)	[16]	3.2	
	PolyALA DP14	235 ($\pm 1.1\%$)	228 ($\pm 3\%$)	[16]	3.1	
	+2	Bradykinin	254 ($\pm 0.8\%$)	246	[32]	3.3
		PolyALA DP13	228 ($\pm 0.7\%$)	220 ($\pm 3\%$)	[16]	3.6
		PolyALA DP14	238 ($\pm 1.8\%$)	232 ($\pm 3\%$)	[16]	2.6
PolyALA DP15		251 ($\pm 1.2\%$)	243 ($\pm 3\%$)	[16]	3.3	
PolyALA DP16		261 ($\pm 0.6\%$)	255 ($\pm 3\%$)	[16]	2.4	
PolyALA DP17		272 ($\pm 1.7\%$)	265 ($\pm 3\%$)	[16]	2.6	
PolyALA DP18		282 ($\pm 0.7\%$)	276 ($\pm 3\%$)	[16]	2.2	
PolyALA DP19		291 ($\pm 1.4\%$)	287 ($\pm 3\%$)	[16]	1.4	
PolyALA DP20		301 ($\pm 1.1\%$)	297 ($\pm 3\%$)	[16]	1.3	
PolyALA DP21		309 ($\pm 0.5\%$)	308 ($\pm 3\%$)	[16]	0.3	
PolyALA DP22		320 ($\pm 1.0\%$)	317 ($\pm 3\%$)	[16]	0.9	
PolyALA DP23		329 ($\pm 0.7\%$)	327 ($\pm 3\%$)	[16]	0.6	
PolyALA DP24		338 ($\pm 1.0\%$)	337 ($\pm 3\%$)	[16]	0.3	
PolyALA DP25		348 ($\pm 0.3\%$)	348 ($\pm 3\%$)	[16]	0	
PolyALA DP26	358 ($\pm 0.7\%$)	358 ($\pm 3\%$)	[16]	0		
Average percentage difference (%)		1.87				

distributions of +2 PolyALA (DP 18) and PEG (DP 20) ions have been recorded under both conditions and are presented in Figure 4. These ions have been selected because of their similar m/z ratios (m/z 649 for +2 PolyALA and m/z 472 for +2 PEG) and CCS (276 \AA^2 for +2 PolyALA and 274 \AA^2 for +2 PEG), and it should be noted that no fragmentation reaction is observed at the higher trap bias voltage.

It is observed that the ATDs of +2 PolyALA ions are slightly shifted when modifying the trap bias voltage, whereas ATDs of PEG ions remain nearly superimposable. This is further confirmed by recording the ATDs of +2 PolyALA (DP 16) and PEG (DP 18) at different trap bias voltages (Supplementary Figure SI 4). The results indicate that PolyALA ions are sensitive to instrumental conditions,

whereas PEG ions remain conformationally stable. The ATD shift for the PolyALA ions could undoubtedly induce errors in a calibration procedure based on PolyALA while the robustness of polymer ions is clearly underlined.

To test further the polymer calibration facing instrumental conditions, a sample of ubiquitin on the Waters Synapt G2-Si has been analyzed under *soft* and *hard* conditions. The typical *soft* conditions are defined as: sampling cone of 10 V, source offset of 50 V, source gas flow of $250 \text{ mL}\cdot\text{min}^{-1}$, desolvation gas flow of $1200 \text{ L}\cdot\text{h}^{-1}$, trap bias voltage of 30 V, and StepWave1 rf offset voltage of 100 V. The *hard* conditions are: sampling cone of 30 V, source offset of 80 V, source gas flow of $0 \text{ mL}\cdot\text{min}^{-1}$, desolvation gas flow of $600 \text{ L}\cdot\text{h}^{-1}$, trap bias voltage of 60 V, and StepWave1 rf offset voltage of 300 V.

Table 2. Reference CCS Compared with CCS Obtained by the Polymer Calibration for +3, +4, and +5 Analytes

Charge state	Analyte	Collision cross-section (\AA^2)			
		Polymer calibration	Reference	Literature reference	Percentage difference (%)
+3	Melittin (Honey Bee)	574 ($\pm 1.0\%$)	581 ($\pm 3\%$)	[33]	1.2
	Insulin (Human)	749 ($\pm 1.6\%$)	757 ($\pm 3\%$)	[33]	1.1
+4	Ubiquitin (Bovine)	969 ($\pm 1.1\%$)	978 ($\pm 1.3\%$)	a	0.9
	Cytochrome <i>c</i> (Bovine)	1181 ($\pm 3.6\%$)	1182 ($\pm 1\%$)	a	0.1
+5	Ubiquitin (Bovine)	1029 ($\pm 1.0\%$)	1007 ($\pm 0.5\%$)	a	2.2
	Average percentage difference (%)		1.1		

Percentages in brackets for Refs [16] and [33] are estimates of the absolute error for the reported measurements

(a) CCS determined in Lyon on a *home-made* DTIMS mass spectrometer

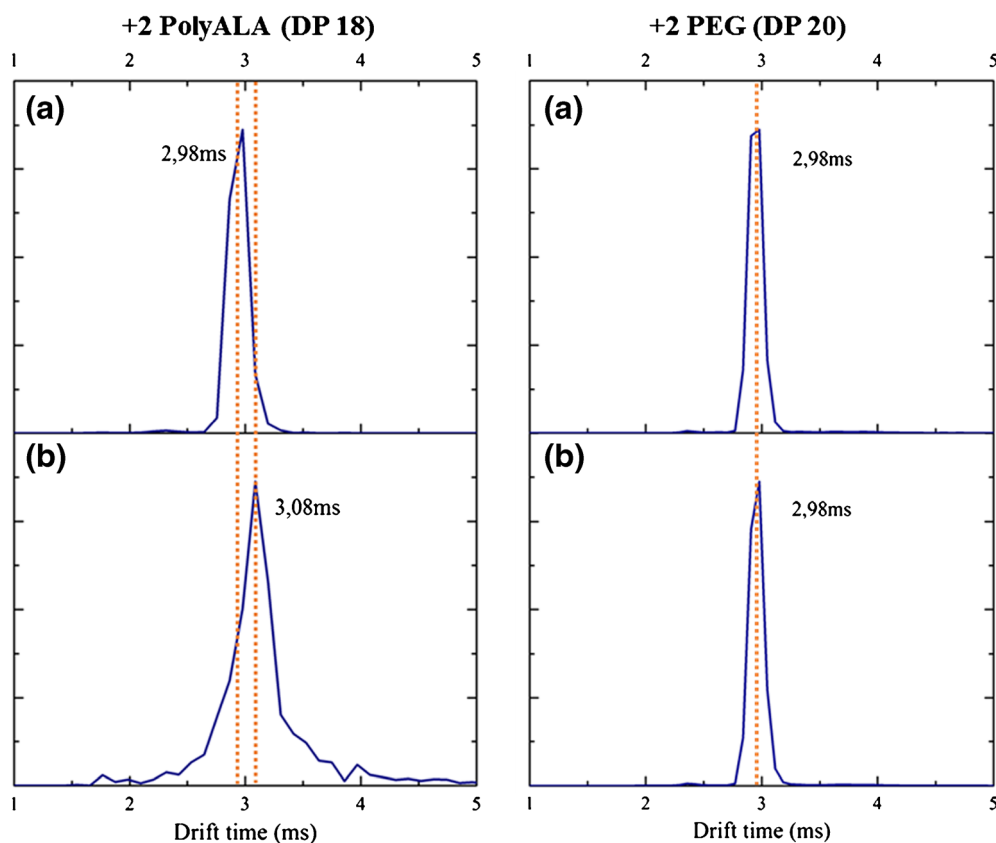


Figure 4. Arrival time distributions of +2 PolyALA (DP 18) and PEG (DP 20) ions with the trap bias voltage at 30 V (a) and 110 V (b)

The polymer calibration must be determined under both conditions; we noticed that the drift times of polymer ions are not significantly different under both conditions regardless of their charge state. The two calibration curves for the +5 ions have similar slopes (lower than 1% of difference between the two slopes) again confirming that polymer ions are not prone to structural modifications upon ion activation (Figure 5).

However, the ATD of the ubiquitin +5 ions is sensitive to the experimental conditions. The ATD have been converted into CCS distributions by means of the polymer calibration

(Supplementary Figure S15). The fact that significant unfolding of protein ions can be evidenced by a collision cross-section distribution obtained by the polymer calibration confirms that protein ions are clearly not suitable as CCS calibrants on a broad range of instrumental conditions. It should also be noted that the CCS obtained (1049 \AA^2 under *soft* and 1130 \AA^2 under *hard* conditions) for +5 native or denatured ubiquitin ions by the polymer calibration correctly match values reported in the literature (i.e., 1027 \AA^2 for native +5 ubiquitin and 1137 \AA^2 for denatured +5 ubiquitin) [20].

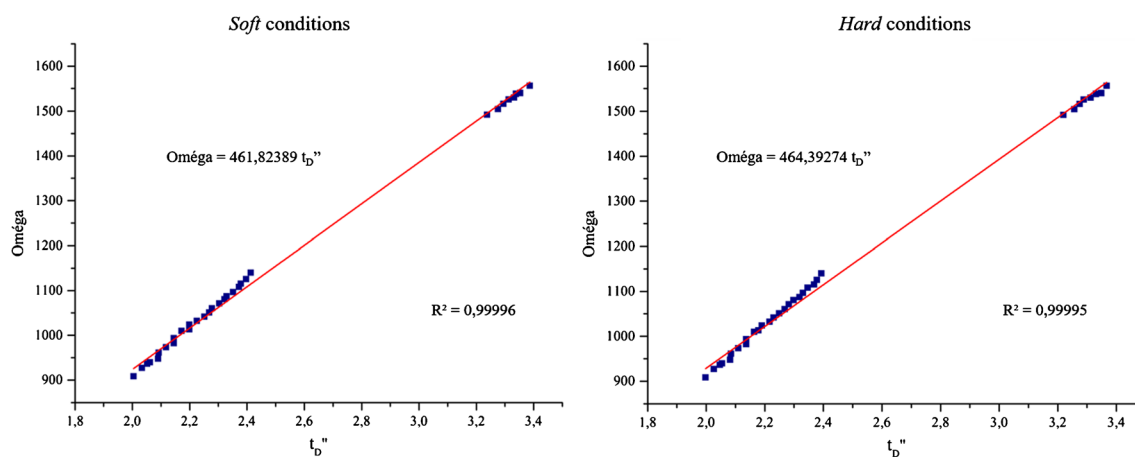


Figure 5. Calibration curves obtained for +5 polymer ions under soft and hard instrumental conditions

Conclusion

In the present paper, we introduce a new method for TWIMS CCS calibration based on the use of polymers as source of calibrant ions. The main motivation is to improve the calibration range and the reliability of available calibration procedures based on the use of PolyALA or other peptide/protein ions as calibrants. Indeed, the dispersity of the polymer samples and their ability to form different charge states upon electrospray analysis allows maximizing the CCS range covered by minimizing the number of samples. Furthermore, polymer ions have been shown to be robust facing a large range of instrumental conditions, confirming their potential for calibration procedure. Synthetic polymers are also inexpensive, straightforward to produce, and stable in solution. Therefore, the use of synthetic polymers as CCS calibrants allows taking a step further towards “perfect” CCS calibrant. For the present purpose, the two investigated polymers were PEG and PLA samples with different averaged molecular weights. We do think that this work opens the door to a better CCS database that aims to be extended with other polymers for higher charge states and broader CCS range. This feature is of particular interest regarding the analysis of large systems such as proteins or biomolecular assemblies that are out of the range of current calibration procedures.

Experimental

Materials

The PEG samples with average molecular weights of 600, 1000, 2000 and 3350 g.mol⁻¹ are commercially available (Sigma Aldrich). The PLA samples are characterized by average molecular weights of 4000, 5500, and 10000 g.mol⁻¹ and are prepared by using the following synthetic procedure:

Typical procedure for PLA ~4000 g.mol⁻¹ synthesis: In a glovebox under nitrogen pressure (O₂ < 5 ppm, H₂O < 1 ppm), a vial is charged with L-LA (1.00 g, 6.9 mmol) and methanol (11 μL, 0.28 mmol). CH₂Cl₂ (10.0 g) is added followed by the addition of 1,8-diazabicyclo[5.4.0]undec-7-ene (DBU, 43 μL, 0.28 mmol). [L-LA]₀/[methanol]₀/[DBU]₀ = 25/1/1. After 3 min of reaction, the polymerization is stopped by addition of an excess of benzoic acid. The polymer is finally recovered by precipitation in cold methanol.

Commercially available samples of quaternary ammonium, reserpine, human insulin, bovine ubiquitin, and bovine cytochrome *c* (Sigma Aldrich) are used without further purification. Bradykinin and melittin are included in the commercially available Waters MassPREP Peptide Mixture. Polyalanine samples are used from the standards kit delivered by Waters.

Sample Preparation for TWIMS and DTIMS Measurements

Polymer solutions are prepared at a final concentration of 15 μM in acetonitrile; 10 μL of sodium iodide solution

(13 mm in acetonitrile) are added to the polymer solution. Quaternary ammonium solutions are prepared at a final concentration of 2 μM in acetonitrile. Reserpine solution is prepared at a final concentration of 10 μM in H₂O/MeOH 1/1; 1 μL of formic acid 99% is added to the reserpine solution. Protein solutions are prepared at a final concentration of 15 μM in an aqueous buffer of ammonium acetate (50 mM). The Waters MassPREP Peptide Mixture is diluted in 1 mL of water to which 2 μL of formic acid 99% are added.

Drift Tube Ion Mobility Spectrometry

The custom DTIMS instrument is described in details elsewhere [26, 27]. It couples an electrospray source, a dual drift tube assembly, and a time-of-flight mass spectrometer (Maxis Impact; Bruker, Bremen, Germany). A constant helium pressure of 4 Torr is maintained in the drift tubes, at a temperature of 300 K. The two drift tubes are 79 cm long, and the typical voltages across the tubes range from 200 to 600 V. For each sample, seven spectra are recorded with voltages between 300 and 500 V to determine the analysis dead time.

DTIMS data are analyzed using custom software developed at the University of Lyon. The dead time correction is determined from a linear regression of the measured arrival times as a function of 1/V (see Equations 1 and 2). After subtraction of the dead time, CCS are calculated from drift times using the Equation of Mason-Schamp (Equation 1).

Traveling Wave Ion Mobility Spectrometry

TWIMS experiments are performed using a Waters Synapt G2-Si mass spectrometer. All the solutions are directly infused in the ESI source with a typical flow rate of 5 μL min⁻¹ with a capillary voltage of 3.1 kV, a source temperature of 100 °C, and a desolvation temperature of 200 °C. Ion mobility (IM) parameters such as traveling wave height, velocity, and gas flow (N₂) in the IM cell are different for each experiment to ensure the robustness of the method. The sets of IM parameters are listed in Table S16.

TWIMS data are analyzed using Waters MassLynx. Arrival time distributions (ATD) are recorded by selecting the most abundant isotope for each polymer ion composition to avoid unspecific selection. Arrival times (t_A) are then determined at the maximum of the ATD.

Acknowledgments

The UMONS MS laboratory acknowledges the Fonds National de la Recherche Scientifique (FRS-FNRS) for its contribution to the acquisition of the Waters Synapt G2-Si mass spectrometer and for continuing support. The authors thank Waters UK (Manchester) for the partnership over the years and particularly, Kirsten Craven, Peter Hancock, and Peter Jenkins. The work in the Laboratory for Chemistry of Novel Materials was supported by the Interuniversity Attraction Pole program of the Belgian Federal Science Policy Office (PAI 7/05), and the Programme d'Excellence de la Région Wallonne (OPTI2MAT

project). J.C. is an FNRS Research Director, O.C. is Research Associate for the FNRS, and Q.D. is a research fellow from FNRS. The IMS experiments in Lyon were performed with funding of European Research Council under the European Union's Seventh Framework Programme (FP7/2007-2013 Grant Agreement no. 320659).

References

- Smith, D.P., Knapman, T.W., Campuzano, I., Malham, R.W., Berryman, J.T., Radford, S.E., Ashcroft, A.E.: Deciphering drift time measurements from traveling wave ion mobility spectrometry-mass spectrometry studies. *Eur. J. Mass Spectrom.* (Chichester, Engl.) **15**, 113–130 (2009)
- McDaniel, E.W., Martin, D.W., Barnes, W.S.: Drift tube-mass spectrometer for studies of low-energy ion-molecule reactions. *Rev. Sci. Instrum.* **33**, 2–7 (1962)
- Lanucara, F., Holman, S.W., Gray, C.J., Eyers, C.E.: The power of ion mobility-mass spectrometry for structural characterization and the study of conformational dynamics. *Nat. Chem.* **6**, 281–294 (2014)
- Shi, L., Holliday, A.E., Glover, M.S., Ewing, M.A., Russell, D.H., Clemmer, D.E.: Ion mobility-mass spectrometry reveals the energetics of intermediates that guide polyproline folding. *J. Am. Soc. Mass Spectrom.* **27**, 22–30 (2016)
- De Winter, J., Lemaure, V., Ballivian, R., Chirot, F., Coulembier, O., Antoine, R., Lemoine, J., Cornil, J., Dubois, P., Dugourd, P., Gerbaux, P.: Size dependence of the folding of multiply charged sodium cationized polylactides revealed by ion mobility mass spectrometry and molecular modeling. *Chem. A Eur. J.* **17**, 9738–9745 (2011)
- Decroo, C., Colson, E., Demeyer, M., Lemaure, V., Caulier, G., Eeckhaut, I., Cornil, J., Flammang, P., Gerbaux, P.: Tackling saponin diversity in marine animals by mass spectrometry: data acquisition and integration. *Anal. Bioanal. Chem.* **409**, 3115–3126 (2017)
- Carroy, G., Lemaure, V., De Winter, J., Isaacs, L., De Pauw, E., Cornil, J., Gerbaux, P.: Energy-resolved collision-induced dissociation of non-covalent ions: charge- and guest-dependence of the decomplexation reaction efficiencies. *Phys. Chem. Chem. Phys.* **18**, 12557–12568 (2016)
- D'Atri, V., Porrini, M.: Linking molecular models with ion mobility experiments. Illustration with a rigid nucleic acid structure. *J. Mass Spectrom.* **50**, 711–726 (2015)
- Mason, E.A., McDaniel, E.W.: Transport properties of ions in gases. John Wiley, New York (1988)
- Pringle, S.D., Giles, K., Wildgoose, J.L., Williams, J.P., Slade, S.E., Thalassinou, K., Bateman, R.H., Bowers, M.T., Scrivens, J.H.: An investigation of the mobility separation of some peptide and protein ions using a new hybrid quadrupole/traveling wave IMS/oa-ToF instrument. *Int. J. Mass Spectrom.* **261**, 1–12 (2007)
- Shvartsburg, A.A., Smith, R.D.: Fundamentals of traveling wave ion mobility spectrometry. *Anal. Chem.* **80**, 9689–9699 (2008)
- Bush, M.F., Hall, Z., Giles, K., Hoyes, J., Robinson, C.V., Ruotolo, B.T.: Collision cross-sections of proteins and their complexes: a calibration framework and database for gas-phase structural biology. *Anal. Chem.* **82**, 9557–9565 (2010)
- Ridenour, W.B., Kliman, M., Mclean, J.A., Caprioli, R.M.: Structural characterization of phospholipids and peptides directly from tissue sections by MALDI Traveling-wave ion mobility-mass spectrometry. *Anal. Chem.* **82**, 1881–1889 (2010)
- Knapman, T.W., Berryman, J.T., Campuzano, I., Harris, S.A., Ashcroft, A.E.: Considerations in experimental and theoretical collision cross-section measurements of small molecules using traveling wave ion mobility spectrometry-mass spectrometry. *Int. J. Mass Spectrom.* **298**, 17–23 (2010)
- Williams, J.P., Bugarcic, T., Habtemariam, A., Giles, K., Campuzano, I., Rodger, P.M., Sadler, P.J.: Isomer separation and gas-phase configurations of organoruthenium anticancer complexes: ion mobility mass spectrometry and modeling. *J. Am. Soc. Mass Spectrom.* **20**, 1119–1122 (2009)
- Bush, M.F., Campuzano, I.D.G., Robinson, C.V.: Ion mobility mass spectrometry of peptide ions: effects of drift gas and calibration strategies. *Anal. Chem.* **84**, 7124–7130 (2012)
- Paglia, G., Angel, P., Williams, J.P., Richardson, K., Olivos, H.J., Thompson, J.W., Menikarachchi, L., Lai, S., Walsh, C., Moseley, A., Plumb, R.S., Grant, D.F., Palsson, B.O., Langridge, J., Geromanos, S., Astarita, G.: Ion mobility-derived collision cross-section as an additional measure for lipid fingerprinting and identification. *Anal. Chem.* **87**, 1137–1144 (2015)
- Forsythe, J.G., Petrov, A.S., Walker, C.A., Allen, S.J., Pellisier, J.S., Bush, M.F., Hud, N.V., Fernandez, F.M.: Collision cross-section calibrants for negative ion mode traveling wave ion mobility-mass spectrometry. *Analyst* **140**, 6853–6861 (2015)
- Allison, T.M., Landreh, M., Benesch, J.L.P., Robinson, C.V.: Low charge and reduced mobility of membrane protein complexes has implications for calibration of collision cross-section measurements. *Anal. Chem.* **88**, 5879–5884 (2016)
- Valentine, S.J., Counterman, A.E., Clemmer, D.E.: Conformer-dependent proton-transfer reactions of ubiquitin ions. *J. Am. Soc. Mass Spectrom.* **8**, 954–961 (1997)
- Hopper, J.T.S., Oldham, N.J.: Collision induced unfolding of protein ions in the gas phase studied by ion mobility-mass spectrometry: the effect of ligand binding on conformational stability. *J. Am. Soc. Mass Spectrom.* **20**, 1851–1858 (2009)
- Merenbloom, S.I., Flick, T.G., Williams, E.R.: How hot are your ions in TWAVE ion mobility spectrometry? *J. Am. Soc. Mass Spectrom.* **23**, 553–562 (2012)
- Poyer, S., Comby-Zerbino, C., Choi, C.M., Macaleese, L., Bogliotti, N., Xie, J., Salpin, J., Dugourd, P., Chirot, F.: Conformational dynamics in ion mobility data. *Anal. Chem.* **89**, 4230–4237 (2017)
- Sun, Y., Vahidi, S., Sowole, M.A., Konermann, L.: Protein structural studies by traveling wave ion mobility spectrometry: a critical look at electrospray sources and calibration issues. *J. Am. Soc. Mass Spectrom.* **27**, 31–40 (2016)
- Duez, Q., Josse, T., Lemaure, V., Chirot, F., Choi, C.M., Dubois, P., Dugourd, P., Cornil, J., Gerbaux, P., De Winter, J.: Correlation between the shape of the ion mobility signals and the stepwise folding process of polylactide ions. *J. Mass Spectrom.* **52**, 133–138 (2017)
- Simon, A.-L., Chirot, F., Choi, C.M., Clavier, C., Barbaire, M., Maurelli, J., Dagany, X., MacAleese, L., Dugourd, P.: Tandem ion mobility spectrometry coupled to laser excitation. *Rev. Sci. Instrum.* **86**, 94101 (2015)
- Choi, C.M., Simon, A.L., Chirot, F., Kulesza, A., Knight, G., Daly, S., MacAleese, L., Antoine, R., Dugourd, P.: Charge, color, and conformation: spectroscopy on isomer-selected peptide ions. *J. Phys. Chem. B* **120**, 709–714 (2016)
- Foley, C.D., Zhang, B., Alb, A.M., Trimpin, S., Grayson, S.M.: Use of ion mobility spectrometry-mass spectrometry to elucidate architectural dispersity within star polymers. *ACS Macro Lett.* **4**, 778–782 (2015)
- Larriba, C., de La Mora, J.F.: The gas phase structure of coulombically stretched polyethylene glycol ions. *J. Phys. Chem. B* **116**, 593–598 (2012)
- Ruotolo, B.T., Benesch, J.L.P., Sandercock, A.M., Hyung, S., Robinson, C.V.: Ion mobility-mass spectrometry analysis of large protein complexes. *Nat. Protoc.* **3**, 1139–1152 (2008)
- Campuzano, I., Bush, M.F., Robinson, C.V., Beaumont, C., Richardson, K., Kim, H., Kim, H.I.: Structural characterization of drug-like compounds by ion mobility mass spectrometry: comparison of theoretical and experimentally derived nitrogen collision cross-sections. *Anal. Chem.* **84**, 1026–1033 (2012)
- Counterman, A.E., Valentine, S.J., Srebalus, C.A., Henderson, S.C., Hoaglund, C.S., Clemmer, D.E.: High-order structure and dissociation of gaseous peptide aggregates that are hidden in mass spectra. *J. Am. Soc. Mass Spectrom.* **9**, 743–759 (1998)
- Salbo, R., Bush, M.F., Naver, H., Campuzano, I., Robinson, C.V., Pettersson, I., Jorgensen, T.J.D., Haselmann, K.F.: Traveling-wave ion mobility mass spectrometry of protein complexes: accurate calibrated collision cross-sections of human insulin oligomers. *Rapid Commun. Mass Spectrom.* **26**, 1181–1193 (2012)